JACS Au
AN OPEN ACCESS JOURNAL OF THE AMERICAN CHEMICAL SOCIETY

pubs.acs.org/jacsau
Article

Spectroscopic Characterization of the 1-Boratricyclo-[4.1.0.0^{2,7}]-heptane Radical with a Delocalized Four-Center-One-Electron Bond

Chuan-Ming Dai,[§] Jiaping Xu,[§] Xin Xu,[§] Cong Wang, Tao You, Wei Li,* and Jiwen Jian*

Cite This: *JACS Au* 2024, 4, 3183−3193
Read Online

ABSTRACT: The boron atom is a highly electrophilic reagent due to the presence of its empty p orbital, making it prone to undergo electrophilic addition reactions with the carbon−carbon double bonds of olefins. In this study, the classical C═C reaction pathway occurs when a boron atom attacks the C═C bond of cyclohexene, resulting in the formation of the η^2 (1,2)-BC_6H_{10} complex (**A**) that contains a borirane radical subunit. This complex can further undergo photoisomerization, leading to the formation of a 3,4,5,6-tetrahydroborepine radical (**C**) through the cleavage of C−C bonds. In addition, two 1-boratricyclo[4.1.0.0^{2,7}]heptane radicals with chair (**B**) and boat (**B′**) conformations were observed through α C−H cleavage reactions. Bonding analysis indicates that these radicals involve a four-center-one-electron (4c-1e) bond. Under UV light irradiation, these two radicals undergo ring-opening and rearrangement reactions, resulting in the formation of a 1-cyclohexen-1-yl-borane radical (**D**), which is a sp^2 C−H activation product. These findings delineate a potential pathway for the synthesis of organoboron radicals through boron-mediated C−H and C−C bond cleavage reactions in cycloolefins.

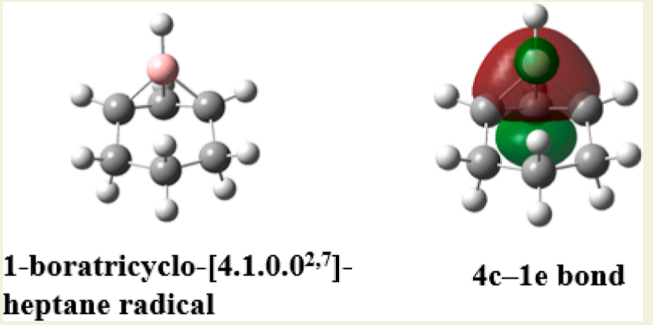

KEYWORDS: *infrared spectrum, matrix isolation, boron, cyclohexene, organoboron radicals*

INTRODUCTION

Metal-catalyzed C−H bond borylation reactions are transition-metal-catalyzed organic reactions that involve the functionalization of C−H bonds to produce organoboron compounds. These reactions have gained significant attention over the past two decades due to their importance in the synthesis of organic materials, natural products, pharmaceuticals, and fine chemicals.[1−14] However, the reliance on precious-metal catalysts with ligands poses limitations, especially in terms of trace-metal residue issues in pharmaceutical products. This has led to the exploration of metal-free catalysts that can mimic the reactivity of metallic systems. In recent years, electron-deficient boron-based catalyst systems have shown promising results in C−H bond transformations.[15−18] These new methodologies have expanded the range of substrates, improved reaction efficiency, and provided new chemical and regioselectivity options. Organoboron intermediates and/or radicals play a key role in the mechanisms of metal-catalyzed and metal-free catalyzed C−H bond borylation reactions.[19−26] These compounds are usually too reactive to be spectroscopically characterized.

The elementary reactions of boron atoms with hydrocarbons can serve as prototypical models to elucidate the reactivity and reaction mechanisms of organoboron compounds. These reactions involve the activation of C−C and C−H bonds in hydrocarbon molecules by atomic boron, leading to the formation of novel organoboron compounds.[27] Gas-phase kinetic[28−30] and crossed molecular beam dynamic investigations,[31−33] as well as matrix isolation spectroscopic studies,[34−37] have provided valuable insights into the reaction mechanisms and intermediates involved in these processes. Matrix isolation infrared spectroscopy, in particular, has been advantageous in studying the reaction mechanisms and intermediates at low temperatures. Previous research has shown that boron atoms can spontaneously and selectively insert into the C═C double bond of ethylene molecules under matrix isolated conditions, rather than the C−H bond with lower activation energy.[38] Boron atom-mediated ring-opening and rearrangement reactions of benzene molecules, leading to the formation of borepinyl radicals and borole derivatives, have also been observed in solid neon.[39] Additionally, the spectroscopic identification of a ground-state boron atom selectively inserting into the C═C double bond of cyclo-

Received: June 9, 2024
Revised: July 31, 2024
Accepted: July 31, 2024
Published: August 9, 2024

https://doi.org/10.1021/jacsau.4c00492
JACS Au 2024, 4, 3183−3193

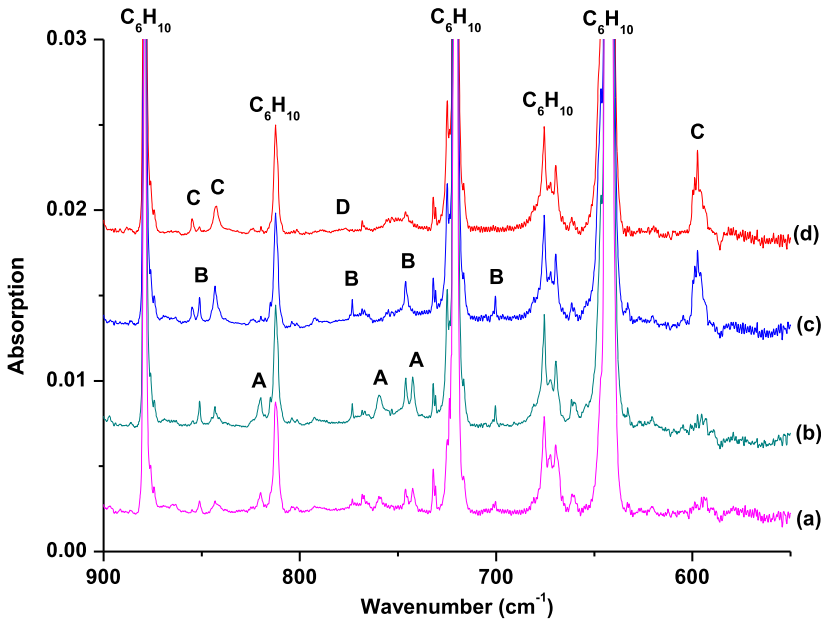

Figure 1. Infrared spectra in the 900−550 cm^{-1} region from codeposition of boron atoms (^{10}B-enriched, 97%) with 0.05% cyclohexene in solid neon: (a) after 30 min deposition at 4 K, (b) after annealing to 12 K, (c) after 15 min $\lambda > 495$ nm UV−visible light irradiation, and (d) after 15 min $\lambda > 280$ nm UV−visible light irradiation.

pentene, forming a 3,4,5-trihydroborinine radical, has been reported in inert matrices.[40] These findings indicate that electron-deficient boron atoms have a tendency to attack molecules with electron-excessive bonds, such as unsaturated bonds in ethylene, allene, acetylene, benzene, and cyclopentene, leading to the formation of novel organoboron compounds.[38−44] However, compared to the activation of unsaturated bonds, the boron-mediated C−H bond activation of unsaturated hydrocarbons has been rarely observed.[15,16,45−47]

Herein, we present a comprehensive study combining matrix isolation infrared spectroscopy and theoretical calculations to investigate the reactions of boron atoms with cyclohexene in solid neon. The aim of this study was to trap and spectroscopically identify the transient intermediates or radicals formed during these reactions as well as to elucidate the boron-mediated C−H and C−C bond activation. The experimental results revealed two distinct reaction pathways involving the activation of both the C═C bond and the C−H bond of cyclohexene by boron atoms. Spectroscopic evidence has been presented for the formation of an η^2 (1,2)-BC_6H_{10} complex (**A**) and a 3,4,5,6-tetrahydroborepine radical (**C**) through the cleavage of the cyclohexene C═C bond. Additionally, the formation of a 1-boratricyclo[4.1.0.0^{2,7}]-heptane radical (**B**) and a 1-cyclohexen-1-yl-borane radical (**D**) through the cleavage of C−H bonds has also been observed. The underlying reaction mechanisms are thoroughly discussed based on quantum chemical calculations.

EXPERIMENTAL AND COMPUTATIONAL METHODS

Since the details of the experimental setup for pulsed laser evaporation and matrix isolation infrared absorption spectroscopy have been previously reported,[48,49] only a short description is provided here. The 1064 nm YAG laser fundamental wavelength (Continuum, Minilite II; 10 Hz repetition rate) was focused onto a rotating boron target to produce the boron atoms. Natural abundance boron (^{10}B, 19.8%; ^{11}B, 80.2%) and ^{10}B-enriched (97%) targets were used in different experiments. The C_6H_{10}/Ne mixtures were prepared in a stainless-steel vacuum line using a standard manometric technique. The C_6H_{10} reagent was used without further purification in the experiment. C_6H_{10} and isotope-labeled C_6D_{10} samples were used. The laser-evaporated boron atoms were codeposited with cyclohexene reagent gas in excess neon onto a cryogenic CsI window, which was maintained at 4 K by employing a closed-cycle helium refrigerator. The samples were usually deposited for 30 min at a rate of approximately 6 mmol/h. The as-deposited samples were subjected to annealing and photolysis experiments to initiate diffusion and photoinduced reactions. Selected samples were also subjected to broadband irradiation using a tungsten lamp or a high-pressure mercury arc lamp with optical filters to initiate further isomerization or dissociation reactions. The infrared absorption spectra of the products in the mid-infrared region (4000−450 cm^{-1}) were recorded on a Bruker Vertex 70 V spectrometer at 0.5 cm^{-1} resolution using a liquid nitrogen-cooled HgCdTe (MCT) detector.

Quantum chemical calculations were performed to determine the molecular structures and to support the assignment of the vibrational frequencies of the observed reaction products. The structural optimization and vibrational frequency computation were done using the three-parameter hybrid functional according to Becke with the correction functional by Lee, Yang, and Parr (B3LYP) with the Gaussian09 program package.[50−52] The Dunning's correlation consistent basis set with polarized triple-ζ plus diffuse functions (aug-cc-pVTZ) has been used for the B, C, and H atoms.[51,53] Single-point calculations were performed at the CCSD(T)/cc-pVTZ level of theory.[54,55] Based on the various possible geometries with different spin states, energy and vibrational calculations were performed to interpret the experimental vibrational features. Transition-state optimizations were performed with the synchronous transit-guided quasi-Newton method and were verified through intrinsic reaction coordinate calculations.[54] Chemical bonding analyses were performed by the adaptive natural density partitioning (AdNDP) method using the density generated from the B3LYP calculations for the assignment of both localized and delocalized bonding using the Multiwfn program.[56,57]

RESULTS AND DISCUSSION

The matrix-isolated products were formed by depositing laser-ablated boron atoms (^{10}B-enriched, 97%) together with 0.05%

https://doi.org/10.1021/jacsau.4c00492
JACS Au 2024, 4, 3183−3193

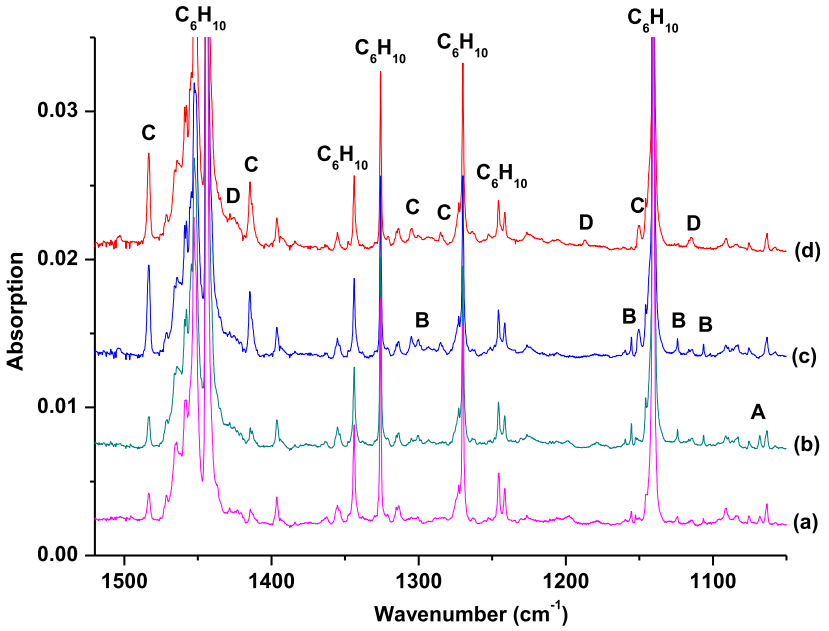

Figure 2. Infrared spectra in the 1520−1050 cm^{-1} region from codeposition of boron atoms (^{10}B-enriched, 97%) with 0.05% cyclohexene in solid neon: (a) after 30 min deposition at 4 K, (b) after annealing to 12 K, (c) after 15 min $\lambda > 495$ nm UV−visible light irradiation, and (d) after 15 min $\lambda > 280$ nm UV−visible light irradiation.

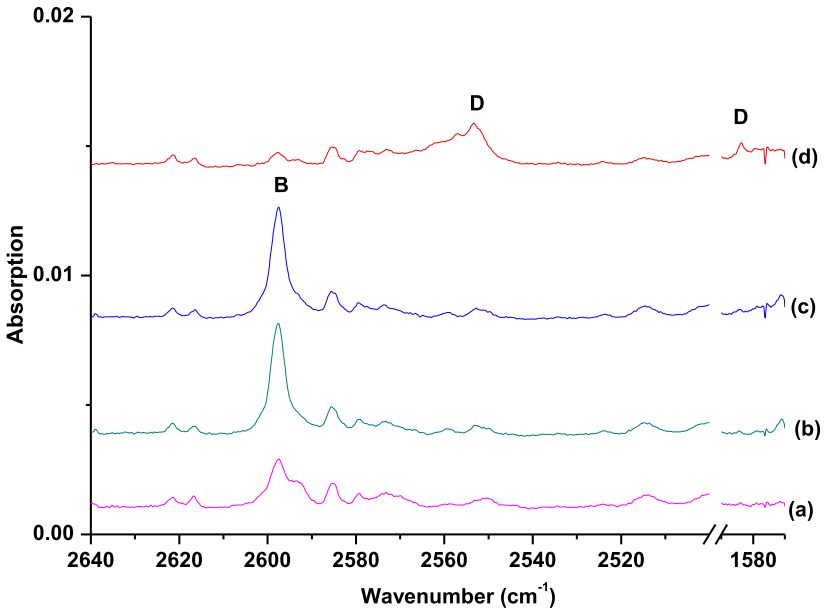

Figure 3. Infrared spectra in the 2640−2500 and 1590−1570 cm^{-1} regions from codeposition of boron atoms (^{10}B-enriched, 97%) with 0.05% cyclohexene in solid neon: (a) after 30 min deposition at 4 K, (b) after annealing to 12 K, (c) after 15 min $\lambda > 495$ nm UV−visible light irradiation, and (d) after 15 min $\lambda > 280$ nm UV−visible light irradiation.

cyclohexene in excess neon. The infrared spectra in selected regions of the reaction products are shown in Figures 1−3. Additionally, Figure S1 shows the spectrum obtained from depositing 0.1% pure cyclohexene in solid argon, which serves as a reference. Besides the strong cyclohexene reactants and residual water absorptions, some new absorptions were observed either upon sample deposition or annealing and photolysis. The product absorptions could be categorized into several groups (labeled as **A**−**D**) based on their annealing and photochemical behaviors. Two new product absorptions (**A** and **B**) appeared on sample deposition and increased on sample annealing. The apparent increase in species **C** was accompanied by the depletion of species **A** when the sample was exposed to broadband irradiation in the wavelength range of $580 > \lambda > 495$ nm using a high-pressure mercury arc lamp. Species **D** was observed under subsequent $580 > \lambda > 280$ nm light irradiation at the cost of species **B**. To aid in product identification based on isotopic shifts, the experiments were repeated under the same conditions using a natural abundance boron target and C_6D_{10} samples. The spectra in selected regions can be seen in Figures 4−5 and S2−S4. The positions of the bands are summarized in Table 1.

Group **A** absorptions are assigned to the different vibrational modes of the η^2 (1,2)-BC_6H_{10} complex, which involves six

https://doi.org/10.1021/jacsau.4c00492
JACS Au 2024, 4, 3183−3193

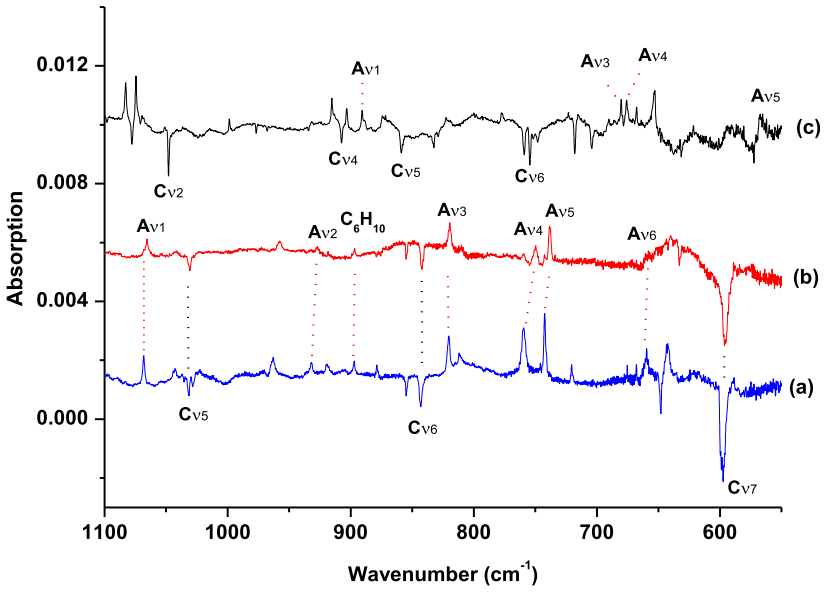

Figure 4. Infrared difference spectra in the 1100−550 cm^{-1} region from codeposition of boron with cyclohexene in solid neon (spectra taken after annealing to 12 K minus spectrum after 15 min $\lambda > 495$ nm UV light irradiation): (a) ^{10}B + 0.05% C_6H_{10}, (b) ^{n}B + 0.05% C_6H_{10}, and (c) ^{10}B + 0.05% C_6D_{10}. The natural abundance boron (^{10}B, 19.8%; ^{11}B, 80.2%) is labeled as ^{n}B. The vibration mode ν_1 of species **A** and **C** is labeled as Aν_1 and Cν_1, respectively.

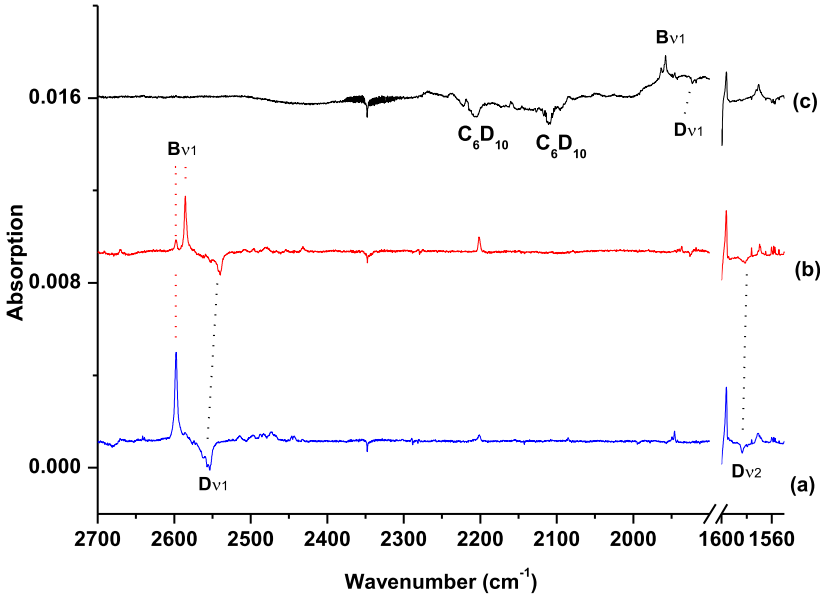

Figure 5. Infrared difference spectra in the 2700−1900 cm^{-1} and 1600−1550 cm^{-1} regions from codeposition of boron with cyclohexene in solid neon (spectra taken after15 min $\lambda > 495$ nm light irradiation minus spectrum after 15 min $\lambda > 280$ nm UV light irradiation): (a) ^{10}B + 0.05% C_6H_{10}, (b) ^{n}B + 0.05% C_6H_{10}, and (c) ^{10}B + 0.05%C_6D_{10}. The natural abundance boron (^{10}B, 19.8%; ^{11}B, 80.2%) is labeled as ^{n}B. The vibration mode ν_1 of species **B** and **D** is labeled as Bν_1 and Dν_1, respectively.

absorptions at 1068.1, 931.7, 819.9, 759.6, 742.5, and 660.2 cm^{-1}. These absorptions are observed on sample deposition and increase on sample annealing at 12 K but markedly decrease on broadband irradiation in the wavelength range of 495−580 nm. The three absorptions at 1068.1, 819.9, and 660.2 cm^{-1} show small boron isotopic shifts mainly ascribed to C−C stretching and/or C−H deformation modes. These band positions are relatively close to those of the cyclohexene oxide complex in solid argon.[58] Two bands at 931.7 and 742.5 cm^{-1} have moderate boron isotopic shifts, suggesting that these bands are assigned to the C−B vibration. The 759.6 cm^{-1} absorption is the most intense band and exhibits the largest boron isotopic shift among the observed absorptions, which is attributed to the C−B vibration.

Group **B** has been identified as the 1-boratricyclo[4.1.0.$0^{2,7}$]-heptane radical. It has two configurations, a chair conformation (**B**) and a boat conformation (**B′**), and different configurations have different characteristic absorptions. These absorptions have similar behavior to group **A** in sample deposition and annealing but remain unchanged when the sample is subjected to 580 > λ > 495 nm UV−visible light irradiation and is almost destroyed under 580 > λ > 280 nm UV−visible light irradiation. Species **B** contains seven absorptions with band centers at 2597.6, 1300.0, 1155.4, 1106.3, 1044.7, 851.1, and

https://doi.org/10.1021/jacsau.4c00492
JACS Au 2024, 4, 3183−3193

Table 1. Comparison of the Observed and Calculated Vibrational Frequencies (ν, cm^{-1}) and Isotopic Shifts (Δ, cm^{-1}) of the $^{10}BC_6H_6$ Isomers

		exptl			calcd		
	modes	ν^a	Δ_B	Δ_H	ν^b	Δ_B	Δ_H
A	ν_1	1068.1 (0.3)	2.6	177.4	1046.4 (13)	3.0	194.0
	ν2	931.7 (0.1)	4.6		940.7 (12)	4.3	184.3
	ν3	819.9 (0.8)	0.2	139.7	808.0 (18)	0.6	140.2
	ν4	759.6 (0.8)	9.9	84.0	741.3 (20)	13.0	96.8
	ν5	742.5 (1.0)	4.3	180.3	733.0 (15)	−0.2	181.4
	ν6	660.2 (0.4)	0.4	59.3	642.8 (15)	1.7	62.2
B	ν1	2597.6 (1.0)	12.1	639.8	2603.9 (105)	12.1	661.0
	ν2	1300.0 (0.1)	1.1	346.6	1275.7 (10)	0.5	352.1
	ν3	1155.4 (0.1)	1.9	301.0	1136.9 (14)	0.8	265.2
	ν4	1106.3 (0.1)	3.9	210.5	1072.6 (12)	4.2	231.0
	ν5	1044.7 (0.1)	—	208.2	1033.3(13)	1.8	216.5
	ν6	851.1 (0.1)	6.5	190.0	842.4 (14)	7.8	156.7
	ν7	746.0 (0.2)	12.2	104.7	734.7 (16)	13.1	103.2
B′	ν1	2597.6 (1.0)	12.1	639.8	2603.2 (100)	12.1	660.2
	ν2	1123.9 (0.1)	1.1	292.6	1108.6 (13)	0.8	245.4
	ν3	—	—	—	1023.9 (16)	2.5	77.9
	ν4	851.1 (0.1)	6.5	14.6	843.9 (13)	5.3	23.4
	ν5	773.3 (0.1)	12.5	125.5	757.3 (14)	8.9	105.8
	ν6	700.4 (0.1)	5.5	102.1	690.2 (10)	5.4	104.2
C	ν1	1483.3 (1.0)	29.0	34.6	1485.6 (53)	31.0	29.1
	ν2	1414.6 (0.8)	10.9	366.6	1405.7 (30)	7.6	369.3
	ν3	1304.9 (0.2)	—	143.0	1294.1 (16)	1.9	176.7
	ν4	1150.3 (0.3)	1.1	242.5	1136.4 (15)	1.4	216.1
	ν5	1031.4 (0.1)	0.9	172.6	1006.0 (12)	0.4	172.3
	ν6	843.3 (0.3)	0.6	88.9	823.9 (13)	0.0	79.9
	ν7	597.4 (0.9)	2.6	—	600.1 (52)	2.7	96.3
D	ν1	2553.3 (1.0)	13.4	630.8	2554.8 (156)	11.3	652.5
	ν2	1583.8 (0.1)	2.3	26.4	1572.3 (86)	0.2	27.5
	ν3	1428.2 (0.1)	0.1	357.4	1412.8 (16)	0.1	379.5
	ν4	1187.0 (0.1)	12.5	63.2	1171.1 (42)	11.7	68.2
	ν5	1115.0 (0.1)	—	202.1	1119.1 (8)	0.3	181.0
	ν6	776.5 (0.1)	—	148.8	762.9 (13)	6.4	143.0

[a]The values in parentheses are the integrated intensities normalized to the most intense absorption. [b]The harmonic vibrational frequencies' scaling factor is 0.968 from the NIST database (NIST-CCCBDB). The calculated IR intensities are listed in parentheses in km/mol. The boron-11 and deuterium isotopic shifts are labeled as Δ_B and Δ_H, respectively.

746.0 cm^{-1}. The absorption band with the highest intensity at 2597.6 cm^{-1} shows very large boron and deuterium isotopic shifts, which are ascribed to the B−H stretching mode. This agrees well with the B−H stretching vibration at the CH_3BH molecule (2561 cm^{-1}) observed in solid argon.[59] The 1300.0, 1155.4, 1106.3, and 1044.7 cm^{-1} bands all exhibit small boron isotopic shifts but large deuterium isotopic shifts that are mainly attributed to the C−H vibrations. The 851.1 and 746.0 cm^{-1} absorptions show large boron and deuterium isotopic shifts, which are indicative of the C−B vibration and B−H deformation mode. The boat conformation radical (**B′**) involves five absorptions at 2597.6, 1123.9, 851.1, 773.3, and 700.4 cm^{-1}. According to the analysis of chair conformation (**B**) and boat conformation (**B′**), species **B′** was presumed to have the same B−H stretching vibration at 2597.6 cm^{-1}. It should be noted that three bands were observed for species **B** and **B′** at the same frequencies of 2597.6, 1044.7, and 851.1 cm^{-1}. These bands are attributed to the vibrations of the BH tricycle subunit. The band at 1123.9 cm^{-1} shows a small boron isotopic shift but a very large deuterium isotopic shift. It is mainly due to C−C and/or C−H vibrations. The observed large boron and deuterium isotopic shifts imply that the 773.3 cm^{-1} band is appropriately assigned to the B−H deformation mode. The 700.4 cm^{-1} band with a small boron isotopic shift but a large deuterium isotopic shift is due to the CH_2 deformation mode, which is in good agreement with the CH_2 deformation mode of $H_2C{=}BH$ (705.7 cm^{-1}).[59]

Species **C** is formed at the cost of species **A** under UV light irradiation, indicating that species **C** results from photoisomerization of species **A**. It is assigned to the 3,4,5,6-tetrahydroborepine radical, for which seven absorptions at 1483.3, 1414.6, 1304.9, 1150.3, 1031.4, 843.3, and 597.4 cm^{-1} are observed. The 1483.3 and 1414.6 cm^{-1} bands with quite large boron isotopic shifts are due to B−C stretching vibrations which agree well with the observed antisymmetric C−B−C stretching vibration of the H_2CBCH_2 molecule in solid neon.[38] In addition, the band at 1414.6 cm^{-1} also has a large deuterium isotopic shift that is attributed to the C−H vibration. In previous research, this assignment was consistent with the CH_2 vibration of H_2CBH_2 (1414.7 cm^{-1}).[59] The other four absorption peaks at 1304.9, 1150.3, 1031.4, and 843.3 cm^{-1} show quite small boron isotopic shifts but large deuterium isotopic shifts, which may be due to C−C or C−H vibrations. The most intense absorption of group **C** is observed at 597.4

https://doi.org/10.1021/jacsau.4c00492
JACS Au 2024, 4, 3183−3193

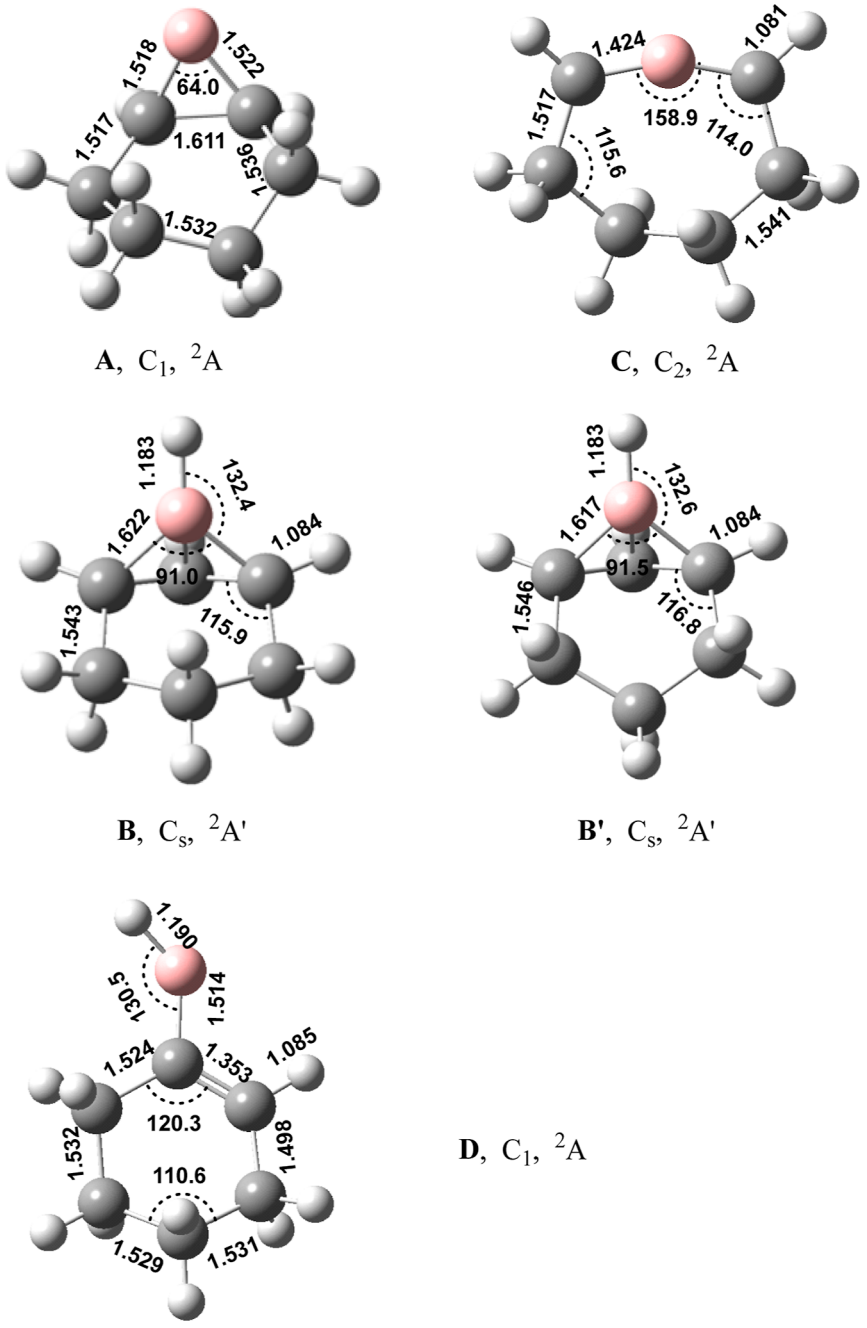

Figure 6. Optimized structures of species **A**–**D** at the B3LYP/aug-cc-pVTZ level (bond lengths in angstrom and bond angles in degrees). Atom colors: B = pink; C = gray; H = white.

cm^{-1}. However, the deuterium isotopic shift is not observed in our infrared spectra because of the large signal-to-noise ratio (S/N) below 500 cm^{-1}.

Species **D** is transformed from group **B** under 580 > λ > 280 nm light irradiation, which involves six absorptions at 2553.3, 1583.8, 1428.2, 1187.0, 1115.0, and 776.5 cm^{-1}. These absorptions are assigned to the different vibrational modes of the 1-cyclohexen-1-yl-borane radical. The 2553.3 cm^{-1} band with quite large boron and deuterium isotopic shifts is due to the B–H stretching vibration, which is similar to species **B**. The band at 1583.8 cm^{-1} shows very small boron and deuterium isotopic shifts; therefore, it is attributed to the C═C stretching vibration. The absorption band at 1187.0 cm^{-1} also shows a large boron isotopic shift, which is indicative of a C–B stretching mode. Besides, the remaining three absorptions at 1428.2, 1115.0, and 776.5 cm^{-1} exhibit relatively large deuterium isotopic shifts, suggesting that they could be mainly attributed to the C–C and/or C–H deformation vibrations.

Following the infrared spectroscopic analysis, we performed theoretical calculations to gain a deeper understanding of the structural, bonding, and mechanistic properties of the five novel radicals formed in the cryogenic matrices. Figure 6 shows the optimized geometries of experimentally observed species **A**–**D** at the B3LYP/aug-cc-pVTZ level.

Species **A** is a transannular π addition complex that possesses a borirane radical subunit and has a ^2A ground state without symmetry. The C–B–C bond angle of the

https://doi.org/10.1021/jacsau.4c00492
JACS Au 2024, 4, 3183–3193

twisted C−B−C subunit is 64.0°. Two different C−B bonds lengths are 1.518 and 1.522 Å, respectively. These geometric parameters are close to those of the C−B−C structure in the BC_2H_4 intermediate.[33] Likewise, a similar cyclohexene oxide cyclic product was considered in the photochemical reaction of cyclohexene with ozone in solid argon.[60]

Species **B** is a tricyclic organoboron radical that possesses two three-membered boron heterocyclic ring moieties and one six-membered boron heterocyclic ring moiety. This compound has two conformational isomers with chair conformation (**B**) and boat conformation (**B′**). Both isomers have the $^2A'$ ground state with C_s symmetry. The calculated B−H bond length of species **B** is 1.183 Å, which is a bit longer than the B−H bond length of the single three-membered borirane ring of the BC_2H_3 product isomers (1.177 Å).[33] It should be noted that the other C−C and C−H bond length and bond angle parameters are in quite good agreement with those of tricyclo[4.1.0.0^{2,7}]heptane.[61] To elucidate the bonding information on species **B**, we performed AdNDP analysis, which has the ability to identify simultaneously both localized and delocalized bonding in chemical species.[62−64] The results are shown in Figure 7, besides 19 2c−2e localized σ bonds (six C−C, nine C−H, three C−B, and one B−H σ bonds), the AdNDP analysis reveals one delocalized 4c−1e bond for the central cyclic-BC_3 moiety.

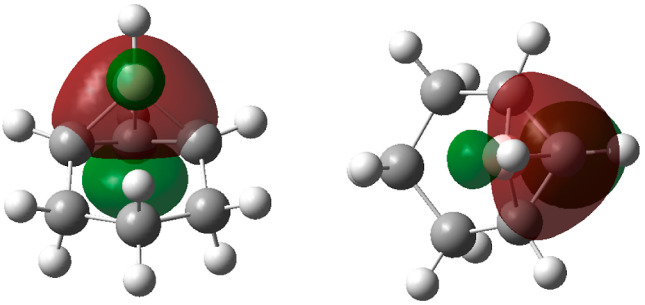

Figure 7. 4c−1e bonds of the 1-boratricyclo[4.1.0.0^{2,7}]heptane radical are illustrated in both top view and side view using AdNDP analysis.

Species **C** with a seven-membered ring has a ^2A ground state and nonplanar C_2 symmetry. The C−B bond length of species **C** is 1.424 Å and fits well with the C−B bond length of 1.425 Å in the H_2CBCH_2 molecule.[38] The C−B−C bond angle is 158.9°, which is slightly larger than that in the 3,4,5-trihydroborinine radical (150.7°).[40] Species **D** is predicted to have a nonplanar structure with a ^2A ground state involving the insertion of a boron atom into the sp^2 C−H bond of cyclohexene. The geometric parameters and spatial configuration of the carbon ring are in good agreement with the previously reported lowest energy conformers of 3-cyclohexen-1-ol at the CCSD/cc-pVTZ level.[65]

As shown in Tables 1 and S1 and S2, it is apparent that the prediction of five BC_6H_{10} isomers' vibration frequencies and intensities shows excellent agreement with the experimental spectrum. For the η^2 (1,2)-BC_6H_{10} complex (**A**), the 741.3 cm^{-1} absorption shows the strongest infrared absorption intensity and the largest boron-11 isotopic shift in the calculation corresponding to the strongest infrared absorption intensity and the largest boron-11 isotopic shift (9.9 cm^{-1}) of species A at 759.6 cm^{-1} observed in the experiment. Regardless of whether it is the standard vibrational frequencies or the isotopic shifts of boron-11 and deuterium, the calculated spectral bands for species **A** are in remarkable concordance with the experimentally observed absorptions. The full set of calculated and experimental frequencies, intensities, and isotopic shifts of species **A** are given in Table S3.

For the 1-boratricyclo[4.1.0.0^{2,7}]heptane radical, the B−H stretching vibration is predicted at 2603.9 cm^{-1} in species **B** with chair conformation and 2603.2 cm^{-1} in species **B′** with boat conformation. Both B−H bands are observed at 2597.6 cm^{-1} in the solid neon. The B−H stretching vibration shows the most intense absorption in both the theoretical calculations and experimental observations for species **B** and **B′**. The 746.0 cm^{-1} band in species **B** shows the largest boron-11 isotopic (12.2 cm^{-1}) and is predicted at 734.7 cm^{-1}. The 773.3 cm^{-1} band in species **B′** shows the largest boron-11 isotopic (12.5 cm^{-1}) and is predicted at 757.3 cm^{-1}. These absorptions are assigned to the B−H deformation mode. The other calculated absorptions and corresponding isotopic shifts of species **B** and **B′** are shown in Tables S4 and S5, which are also in good agreement with the experimental observation.

For the 3,4,5,6-tetrahydroborepine radical (**C**), the antisymmetric C−B−C stretching vibration observed at 1483.3 cm^{-1} is predicted at 1485.6 cm^{-1}. This band shows the most intense absorption and largest boron-11 isotopic shift in the calculation (32.0 cm^{-1}) corresponding to the strongest absorption band with a 29.0 cm^{-1} boron-11 isotopic shift. The experimentally observed peak at 1414.6 cm^{-1} is theoretically predicted at 1405.7 cm^{-1}. This absorption is

Scheme 1. Observed Pathways of the Reactions of Boron Atoms with Cyclohexene in Solid Neon[a]

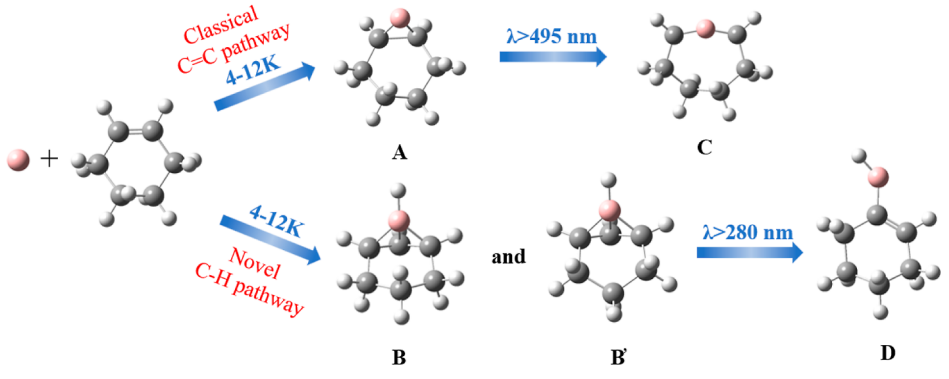

[a]Atom colors: B = pink; C = gray; H = white.

https://doi.org/10.1021/jacsau.4c00492
JACS Au 2024, 4, 3183−3193

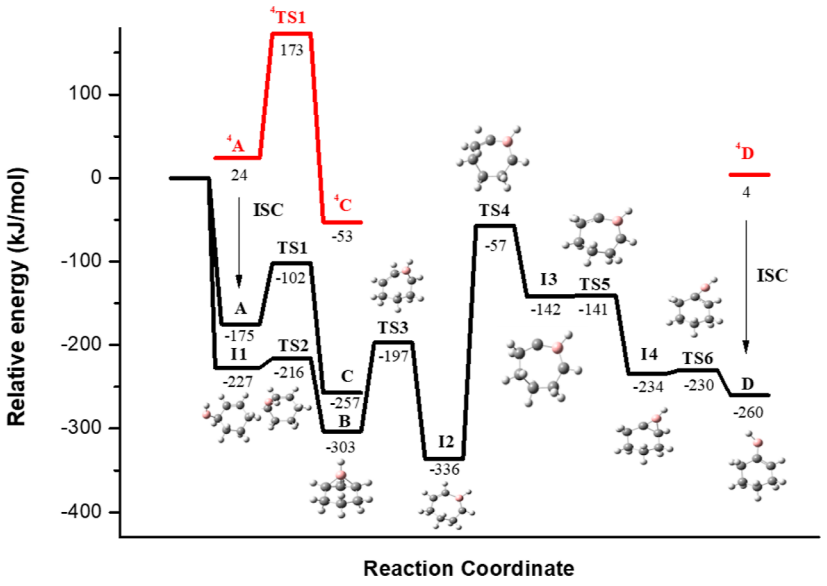

Figure 8. Potential energy profile of the B (^{2}P) + C_6H_{10} reaction calculated at the CCSD(T)/cc-pVTZ//B3LYP/aug-cc-pVTZ level of theory. The energies are expressed in kJ/mol, and the excited-state reactants and products are highlighted in red. ISC stands for intersystem crossing.

ascribed to the C−B−C stretching vibration combined with the C−H scissoring vibration. The full sets of frequencies, intensities, and isotopic shifts are shown in Table S6.

For the 1-cyclohexen-1-yl-borane radical (**D**), the 2553.3 cm^{-1} band shows the largest boron-11 (13.4 cm^{-1}) and deuterium (630.8 cm^{-1}) isotopic shifts predicted at 2554.8 cm^{-1}, which is ascribed to the B−H stretching vibration. It is necessary to point out that the 1583.8 cm^{-1} bands with very small boron-11 (2.3 cm^{-1}) and deuterium (26.4 cm^{-1}) isotopic shifts are attributed to the C═C stretching vibration. This absorption is predicted at 1572.3 cm^{-1}. As shown in Table S7, the other experimental frequencies of species **D** also exhibit good agreement with the theoretical prediction.

Further support for the assignment comes from the nice match between the calculated and experimental isotope shifts; species **A**, **B**, **B′**, **C**, and **D** are safely and correctly assigned (Tables S1 and S2). As shown in Scheme 1, the experimental results point to two reaction pathways involving boron-mediated C═C and C−H activations of cyclohexene, respectively. Figure 8 shows the detailed potential energy profile for the reaction of B (^{2}P) atoms with cyclohexene to generate species **A**, **B**, **C**, and **D** that was calculated at the CCSD(T)/cc-pVTZ//B3LYP/aug-cc-pVTZ level. The T1 diagnoses for the CCSD(T) calculations of species **A**−**D** have been added in Table S10. The C═C double bond activation reaction is initiated by a boron atom attacking the C═C bond of cyclohexene, forming an η^2 (1,2)-BC_6H_{10} complex (**A**) which possesses a borirane radical subunit. This cycloaddition reaction is exothermic by 175 kJ mol^{-1} and exhibits no energy barrier. The η^2 (1,2)-BC_6H_{10} complex (**A**) rearranges to the inserted 3,4,5,6-tetrahydro-borepine radical (**C**) isomer via a transition state (**TS1**) located 73 kJ mol^{-1} above the species **A** structure. In contrast to the η^2 (1,2)-BC_5H_8 complex that cannot be trapped in solid neon due to only 39 kJ mol^{-1} energy barrier, the η^2 (1,2)-BC_6H_{10} complex was observed in the experiment with a calculated 73 kJ mol^{-1} isomerization energy barrier.[40] Species **A** overcomes the energy barrier to generate species **C** under 495−580 nm light irradiation. The reaction to yield species **C** is exothermic by 257 kJ mol^{-1}. The experimental observations and theoretical calculations of the formation of species **A** and **C** are in good agreement. The quartet state products **A**, **B**, **C**, and **D** are indicated in the red line. Given the challenge in trapping higher energy excited-state species in matrix isolation experiments, only the doublet states of **A**, **B**, **C**, and **D** are considered in the photoinduced isomer reactions. Isomerization intermediates formed in other excited states are not considered.

For the C−H bond activation, the reaction is predicted to proceed through a pathway that the boron atom first attacks the α C−H bond of cyclohexene forming an intermediate (**I1**), and then the BH subunit approaches the cyclohexene C═C bond generating the 1-boratricyclo[4.1.0.0^{2,7}]heptane radical (**B**). The reaction to yield species **B** is exothermic by 303 kJ mol^{-1}. However, the energy barrier of intermediate (**I1**) isomerizing to species **B** is only 11 kJ mol^{-1}. This may be the reason that intermediate (**I1**) cannot be trapped and observed in our experiment. However, it is possible that species **B** could also arise from the conversion of species **A**, potentially involving the transfer of hydrogen from sp^3 or sp^2 C−H bonds, as depicted in Figure S5.

The rearrangement reaction from species **B** to the 1-cyclohexen-1-yl-borane radical (**D**) is quite complicated and involves several intermediates and corresponding transition states. First, species **B** rearranges to a seven-membered ring 2,3,4,-trihydro-1*H*-borepine radical intermediate (**I2**) via a transition state (**TS3**) located 106 kJ mol^{-1} above the species **B** structure. This reaction step is in agreement with the previous reports that the benzvalyne and 3-aza-benzvalene compounds isomerize to benzyne and pyridine, respectively, through a ring-expansion reaction.[66−68] The largest energy barrier of the isomerization reaction is 279 kJ mol^{-1}, which undergoes a transition state (**TS4**) to yield an intermediate (**I3**). This is the reason that species **D** was observed only under broadband UV light irradiation. Although intermediate **I2** is kinetically stable due to the large barriers for its isomerization with either **B** or intermediate **I3**, it was not observed in the experiment. The calculated vibrational frequencies, intensities, and corresponding isotopic vibrational frequencies of intermediate **I2** have been included in the Supporting Information (Tables S8 and S9). As shown in Figures S6 and S7, the

https://doi.org/10.1021/jacsau.4c00492
JACS Au 2024, 4, 3183−3193

calculated electronic absorption spectrum of intermediate **I2** indicates its sensitivity to 280−580 nm UV light irradiation, potentially causing the photoisomerization of intermediate **I2** to intermediate **I3**. This may be the reason that intermediate **I2** was not observed in 280−580 nm UV light irradiation.

Intermediate **I4** isomerizes to species **D** through the carbon−boron bond cleavage of the borirane subunit. Since the highest transition state (**TS4**) lies 57 kJ mol^{-1} lower in energy than the ground-state reactants boron atom with cyclohexene, this isomerization reaction is predicted to be both thermodynamically favorable and kinetically facile. The optimized geometries of the corresponding intermediates and transition states are shown in Figures S8 and S9.

The results indicate that atomic boron is quite reactive toward cyclohexene molecules in forming novel organoboron radicals through boron-mediated C═C double bonding and C−H cleavage reactions. The boron atom attacks the C═C double bond of cyclohexene forming a η^2 (1,2)-BC_6H_{10} complex (**A**), which rearranges to the inserted 3,4,5,6-tetrahydro-borepine radical (**C**). This reaction pathway is in perfect match with previous research on the reaction of boron atoms with ethylene,[38] benzene,[39] and cyclopentene.[40] The observation of the 1-boratricyclo[4.1.0.$0^{2,7}$] heptane radical (**B**) and 1-cyclohexen-1-yl-borane radical (**D**) indicates that the C−H bonds are activated by atomic boron. It should be pointed out that the boron atom attacks the α C−H bond of cyclohexene, resulting in forming species **B**. Notice that species **D** is a boron-mediated cyclohexene sp^2 C−H activation product. The spin density is mainly located on the boron atom. Therefore, species **D** is a cyclohexene-substituted borane radical which is named as the 1-cyclohexen-1-yl-borane radical. These boron atom-mediated α C−H bond and sp^2 C−H bond cleavage reactions provide new insights into the directed C−H borylation of unsaturated hydrocarbons and cycloolefins without the use of metal catalysts.

CONCLUSIONS

The reactions of atomic boron with cyclohexene molecules in solid neon have been investigated by using matrix isolation infrared absorption spectroscopy. The experimental results concur with two reaction pathways, where boron-mediated C═C bond and C−H bond activations of cyclohexene take place, respectively. For the C═C double bond activation reaction, the ground-state boron atom attacks the C═C bond of cyclohexene forming an η^2 (1,2)-BC_6H_{10} complex (**A**) which further isomerizes to a 3,4,5,6-tetrahydroborepine radical (C) through C−C bond cleavage under UV light irradiation. For the C−H bond activation reaction, it is predicted to proceed through a pathway that the boron atom first attacks the α C−H bond of cyclohexene forming an intermediate (**I1**), and then the BH subunit approaches the cyclohexene C═C bond, generating the unprecedented 1-boratricyclo[4.1.0.$0^{2,7}$]heptane radical. It is worth highlighting that the chair (**B**) and boat (**B′**) conformers of this radical were both observed in our experiments. These two radicals isomerize to 1-cyclohexen-1-yl-borane radical (**D**), an sp^2 C−H activation product, via ring-opening and rearrangement reactions under UV light irradiation. This is a good example of forming novel organoboron radicals through the boron-mediated C−H and C═C double bond activation of unsaturated hydrocarbons. It is crucial to acknowledge the observed variance in reactivity between cyclopentene and cyclohexene with boron atoms, a phenomenon that remains to be fully elucidated. The present findings provide a possible route for the future design and synthesis of corresponding organoboron radicals through the reactions between atomic boron and cycloolefins.

ASSOCIATED CONTENT

Supporting Information

The Supporting Information is available free of charge at https://pubs.acs.org/doi/10.1021/jacsau.4c00492.

Observed and calculated frequencies of species **A**−**D**, net C_6H_{10} and isotopic infrared spectra of species **A**−**D**, calculated potential energy profile, electronic absorptions spectra, intermediates and transition states, and calculated atomic coordinates (PDF)

AUTHOR INFORMATION

Corresponding Authors

Wei Li − *School of Mathematics and Physics, North China Electric Power University, Beijing 102206, People's Republic of China*; Email: weil@ncepu.edu.cn

Jiwen Jian − *Hangzhou Institute of Advanced Studies, Zhejiang Normal University, Hangzhou, Zhejiang 311231, People's Republic of China*; orcid.org/0000-0002-9268-1987; Email: jiwenjian@zjnu.edu.cn

Authors

Chuan-Ming Dai − *Hangzhou Institute of Advanced Studies, Zhejiang Normal University, Hangzhou, Zhejiang 311231, People's Republic of China*

Jiaping Xu − *Hangzhou Institute of Advanced Studies, Zhejiang Normal University, Hangzhou, Zhejiang 311231, People's Republic of China*

Xin Xu − *Hangzhou Institute of Advanced Studies, Zhejiang Normal University, Hangzhou, Zhejiang 311231, People's Republic of China*

Cong Wang − *Hangzhou Institute of Advanced Studies, Zhejiang Normal University, Hangzhou, Zhejiang 311231, People's Republic of China*

Tao You − *Hangzhou Institute of Advanced Studies, Zhejiang Normal University, Hangzhou, Zhejiang 311231, People's Republic of China*

Complete contact information is available at: https://pubs.acs.org/10.1021/jacsau.4c00492

Author Contributions

[§]C.-M.D., J.X., and X.X. contributed equally.

Notes

The authors declare no competing financial interest.

ACKNOWLEDGMENTS

We gratefully acknowledge the financial support from the National Natural Science Foundation of China (grant nos. 22273089 and 21903069). J.J. also acknowledges the startup fund from the Zhejiang Normal University. We acknowledge Prof. Bin-Bin Xie and Prof. Mingfei Zhou for calculation support and insightful discussions during the development of this work.

REFERENCES

(1) Bisht, R.; Haldar, C.; Hassan, M. M.; Hoque, M. E.; Chaturvedi, J.; Chattopadhyay, B. Metal-catalysed C-H bond activation and borylation. *Chem. Soc. Rev.* **2022**, *51*, 5042−5100.

(2) Oeschger, R.; Su, B.; Yu, I.; Ehinger, C.; Romero, E.; He, S.; Hartwig, J. Diverse functionalization of strong alkyl C-H bonds by undirected borylation. *Science* **2020**, *368*, 736−741.

(3) Xu, L.; Wang, G.; Zhang, S.; Wang, H.; Wang, L. H.; Liu, L.; Jiao, J.; Li, P. F. Recent advances in catalytic C-H borylation reactions. *Tetrahedron* **2017**, *73*, 7123−7157.

(4) Li, Y. Y.; Pang, H. L.; Wu, D.; Li, Z. Q.; Wang, W.; Wei, H.; Fu, Y.; Yin, G. Y. Nickel-catalyzed 1,1-alkylboration of electronically unbiased terminal alkenes. *Angew. Chem., Int. Ed.* **2019**, *58*, 8872−8876.

(5) Hassan, M. M.; Guria, S.; Dey, S.; Das, J.; Chattopadhyay, B. Transition metal-catalyzed remote C-H borylation: An emerging synthetic tool. *Sci. Adv.* **2023**, *9*, No. eadg3311.

(6) Haldar, C.; Hoque, M. E.; Chaturvedi, J.; Hassan, M. M.; Chattopadhyay, B. Ir-catalyzed proximal and distal C-H borylation of arenes. *Chem. Commun.* **2021**, *57*, 13059−13074.

(7) Hoque, M. E.; Hassan, M. M.; Chattopadhyay, B. Remarkably Efficient Iridium Catalysts for Directed C(sp^2)-H and C(sp^3)-H Borylation of Diverse Classes of Substrates. *J. Am. Chem. Soc.* **2021**, *143*, 5022−5037.

(8) Bisht, R.; Chattopadhyay, B. Formal Ir-Catalyzed Ligand-Enabled Ortho and Meta Borylation of Aromatic Aldehydes via in Situ-Generated Imines. *J. Am. Chem. Soc.* **2016**, *138*, 84−87.

(9) Chaturvedi, J.; Haldar, C.; Bisht, R.; Pandey, G.; Chattopadhyay, B. Meta Selective C-H Borylation of Sterically Biased and Unbiased Substrates Directed by Electrostatic Interaction. *J. Am. Chem. Soc.* **2021**, *143*, 7604−7611.

(10) Mahamudul Hassan, M. M.; Mondal, B.; Singh, S.; Haldar, C.; Chaturvedi, J.; Bisht, R.; Sunoj, R. B.; Chattopadhyay, B. Ir-Catalyzed Ligand-Free Directed C-H Borylation of Arenes and Pharmaceuticals: Detailed Mechanistic Understanding. *J. Org. Chem.* **2022**, *87*, 4360−4375.

(11) Hartwig, J. F.; Larsen, M. A. Undirected, Homogeneous C-H Bond Functionalization: Challenges and Opportunities. *ACS Cent. Sci.* **2016**, *2*, 281−292.

(12) Hoque, M. E.; Bisht, R.; Unnikrishnan, A.; Dey, S.; Mahamudul Hassan, M. M.; Guria, S.; Rai, R. N.; Sunoj, R. B.; Chattopadhyay, B. Iridium-Catalyzed Ligand-Controlled Remote para-Selective C-H Activation and Borylation of Twisted Aromatic Amides. *Angew. Chem., Int. Ed.* **2022**, *61*, 1−10.

(13) Hoque, M. E.; Bisht, R.; Haldar, C.; Chattopadhyay, B. Noncovalent Interactions in Ir-Catalyzed C-H Activation: L-Shaped Ligand for Para-Selective Borylation of Aromatic Esters. *J. Am. Chem. Soc.* **2017**, *139*, 7745−7748.

(14) Guria, S.; Hassan, M. M.; Ma, J. W.; Dey, S.; Liang, Y.; Chattopadhyay, B. A tautomerized ligand enabled meta selective C-H borylation of phenol. *Nat. Commun.* **2023**, *14*, 6906.

(15) Li, Y. H.; Wu, X. F. Direct C-H Bond Borylation of (Hetero)Arenes: Evolution from Noble Metal to Metal Free. *Angew. Chem., Int. Ed.* **2020**, *59*, 1770−1774.

(16) Légaré, M. A.; Courtemanche, M. A.; Rochette, E.; Fontaine, F. G. Metal-free catalytic C-H bond activation and borylation of heteroarenes. *Science* **2015**, *349*, 513−516.

(17) Wang, X.; Studer, A. Metal-Free Direct C-H Cyanation of Alkenes. *Angew. Chem., Int. Ed.* **2018**, *57*, 11792−11796.

(18) Lv, J. H.; Chen, X. Y.; Xue, X. S.; Zhao, B.; Liang, Y.; Wang, M. Y.; Jin, L. Q.; Yuan, Y.; Han, Y.; Zhao, Y.; Lu, Y.; Zhao, J.; Sun, W. Y.; Houk, K. N.; Shi, Z. Z. Metal-free directed sp^2-C-H borylation. *Nature* **2019**, *575*, 336−340.

(19) Yang, K.; Song, Q. L. Tetracoordinate Boron Intermediates Enable Unconventional Transformations. *Acc. Chem. Res.* **2021**, *54*, 2298−2312.

(20) Kim, J. H.; Constantin, T.; Simonetti, M.; Llaveria, J.; Sheikh, N. S.; Leonori, D. A radical approach for the selective C-H borylation of azines. *Nature* **2021**, *595*, 677−683.

(21) Vantourout, J. C.; Miras, H. N.; Isidro-Llobet, A.; Sproules, S.; Watson, A. J. B. Spectroscopic Studies of the Chan-Lam Amination: A MechanismInspired Solution to Boronic Ester Reactivity. *J. Am. Chem. Soc.* **2017**, *139*, 4769−4779.

(22) Rej, S.; Chatani, N. Transient Imine as a Directing Group for the Metal-Free o-C-H Borylation of Benzaldehydes. *J. Am. Chem. Soc.* **2021**, *143*, 2920−2929.

(23) Manna, S.; Das, K. K.; Nandy, S.; Aich, D.; Paul, S.; Panda, S. A new avenue for the preparation of organoboron compounds via nickel catalysis. *Coord. Chem. Rev.* **2021**, *448* (214165), 214165.

(24) Hartwig, J. F. Borylation and silylation of C-H bonds: a platform for diverse C-H bond functionalizations. *Acc. Chem. Res.* **2012**, *45*, 864−873.

(25) Liu, Z.; Liu, J.; Mateti, S.; Zhang, C.; Zhang, Y.; Chen, L.; Wang, J.; Wang, H.; Doeven, E. H.; Francis, P. S.; Barrow, C. J.; Du, A. J.; Chen, Y.; Yang, W. Boron Radicals Identified as the Source of the Unexpected Catalysis by Boron Nitride Nanosheets. *ACS Nano* **2019**, *13*, 1394−1402.

(26) Mills, H. A.; Martin, J. L.; Rheingold, A. L.; Spokoyny, A. M. Oxidative Generation of Boron-Centered Radicals in Carboranes. *J. Am. Chem. Soc.* **2020**, *142*, 4586−4591.

(27) Balucani, N.; Zhang, F. T.; Kaiser, R. I. Elementary Reactions of Boron Atoms with Hydrocarbons Toward the Formation of Organo-Boron Compounds. *Chem. Rev.* **2010**, *110*, 5107−5127.

(28) Zhaunerchyk, V.; Vigren, E.; Geppert, W. D.; Hamberg, M.; Danielsson, M.; Kaminska, M.; Larsson, M.; Thomas, R. D.; Bahati, E.; Vane, C. R. Dissociative recombination of BH_2^+: The dominance of two-body breakup and an understanding of the fragmentation. *Phys. Rev. A* **2008**, *78* (2), 024701.

(29) Geppert, W. D.; Goulay, F.; Naulin, C.; Costes, M.; Canosa, A.; Le Picard, S. D.; Rowe, B. R. Rate coefficients and integral cross-sections for the reaction of B (^2P_J) atoms with acetylene. *Phys. Chem. Chem. Phys.* **2004**, *6*, 566−571.

(30) Canosa, A.; Le Picard, S. D.; Geppert, W. D. Experimental Kinetics Study of the Reaction of Boron Atoms B (^2P_J), with Ethylene at Very Low Temperatures (23−295 K). *J. Phys. Chem. A* **2004**, *108*, 6183−6185.

(31) Balucani, N.; Asvany, O.; Lee, Y. T.; Kaiser, R. I.; Galland, N.; Hannachi, Y. Observation of Borirene from Crossed Beam Reaction of Boron Atoms with Ethylene. *J. Am. Chem. Soc.* **2000**, *122*, 11234−11235.

(32) Kaiser, R. I.; Bettinger, H. F. Gas-Phase Detection of the Elusive Benzoborirene Molecule. *Angew. Chem., Int. Ed.* **2002**, *41*, 2350−2352.

(33) Zhang, F.; Gu, X.; Kaiser, R. I.; Balucani, N.; Huang, C. H.; Kao, C. H.; Chang, A. H. H. A Crossed Beam and Ab Initio Study of the Reaction of Atomic Boron with Ethylene. *J. Phys. Chem. A* **2008**, *112*, 3837−3845.

(34) Martin, M. L.; Taylor, P. R.; Hassanzadeh, P.; Andrews, L. Boron Atom Reactions with Acetylene. Ab Initio Calculated and Observed Isotopic Infrared Spectra of the Borirene Radical BC_2H_2. A Fingerprint Match. *J. Am. Chem. Soc.* **1993**, *115*, 2510−2511.

(35) Hassanzadeh, P.; Andrews, L. Reactions of pulsed laser evaporated boron atoms with methane. 1. Synthesis and characterization of a novel molecule with carbon-boron double bonds: HBCBH. *J. Am. Chem. Soc.* **1992**, *114*, 9239−9240.

(36) Andrews, L.; Lanzisera, D. V.; Hassanzadeh, P.; Hannachi, Y. Reactions of Laser-Ablated Boron Atoms with Ethylene and Ethane. Infrared Spectra and DFT Calculations for Several Novel BC_2H_x (x = 1, 2, 3, 4, 5) Molecules. *J. Phys. Chem. A* **1998**, *102*, 3259−3267.

(37) Hassanzadeh, P.; Hannachi, Y.; Andrews, L. Pulsed Laser Evaporated Boron Atom Reactions with Methane. 2. Infrared Spectra of H_2CBH_2, H_2CBH, HCBH, and HBCBH in Solid Argon. *J. Phys. Chem.* **1993**, *97*, 6418−6424.

(38) Jian, J. W.; Lin, H. L.; Luo, M. B.; Chen, M. H.; Zhou, M. F. Observation of Spontaneous C = C Bond Breaking in the Reaction between Atomic Boron and Ethylene in Solid Neon. *Angew. Chem., Int. Ed.* **2016**, *55*, 8371−8374.

https://doi.org/10.1021/jacsau.4c00492
JACS Au 2024, 4, 3183−3193

(39) Jian, J. W.; Wu, X.; Chen, M. H.; Zhou, M. F. Boron-Mediated Carbon-Carbon Bond Cleavage and Rearrangement of Benzene Forming the Borepinyl Radical and Borole Derivatives. *J. Am. Chem. Soc.* **2020**, *142*, 10079−10086.
(40) Xu, J. P.; Xu, X.; Li, D. Y.; Jian, J. W. Spectroscopic characterization of two boron heterocyclic radicals in the solid neon matrix. *Phys. Chem. Chem. Phys.* **2022**, *24*, 7961−7968.
(41) Lanzisera, D. V.; Hassanzadeh, P.; Hannachi, Y.; Andrews, L. Identification of the Borirene Molecule, $(CH)_2BH$: Matrix Isolation FTIR and DFT Calculations for Five Vibrational Modes of Six Isotopic Molecules. *J. Am. Chem. Soc.* **1997**, *119*, 12402−12403.
(42) Maksyutenko, P.; Zhang, F.; Kim, Y. S.; Kaiser, R. I.; Chen, S. H.; Wu, C. C.; Chang, A. H. H. Untangling the Chemical Dynamics of the Reaction of Boron Atoms, $^{11}B(^2P_j)$, with Diacetylene, $C_4H_2(X^1\Sigma_g^+)$—A Crossed Molecular Beams and Ab Initio Study. *J. Phys. Chem. A* **2010**, *114*, 10936−10943.
(43) Zhang, F.; Sun, H. L.; Chang, A. H. H.; Gu, X.; Kaiser, R. I. Crossed Molecular Beam Study on the Reaction of Boron Atoms, $B(^2P_j)$, with Allene, $H_2CCCH_2(XA_1)$. *J. Phys. Chem. A* **2007**, *111*, 13305−13310.
(44) Zhang, F.; Guo, Y.; Gu, X.; Kaiser, R. I. A Crossed Molecular Beam Study on the Reaction of Boron Atoms, $B(^2P_j)$, with Benzene, $C_6H_6(X^1A_{1g})$, and D6-Benzene $C_6D_6(X^1A_{1g})$. *Chem. Phys. Lett.* **2007**, *440*, 56−63.
(45) Lv, J. H.; Zhao, B. L.; Yuan, Y.; Han, Y.; Shi, Z. Z. Boron-mediated directed aromatic C-H hydroxylation. *Nat. Commun.* **2020**, *11*, 1316.
(46) Osi, A.; Mahaut, D.; Tumanov, N.; Fusaro, L.; Wouters, J.; Champagne, B.; Chardon, A.; Berionni, G. Taming the Lewis Superacidity of Non-Planar Boranes: C-H Bond Activation and Non-Classical Binding Modes at Boron. *Angew. Chem., Int. Ed.* **2022**, *61*, No. e202112342.
(47) Scheschkewitz, D.; Amseis, P.; Geiseler, G.; Massa, W.; Hofmann, M.; Berndt, A. Classical 1,2,4-Triboracyclopentanes and Their Rearrangement into Nonclassical 2-Boryl-1,3-diboracyclobutanes: Intramolecular C-H Bond Activation by a B-B Moiety. *Eur. J. Inorg. Chem.* **2005**, *2005*, 4078−4085.
(48) Wang, G. J.; Zhou, M. F. Probing the Intermediates in the MO + CH_4 ↔ M + CH_3OH Reactions by Matrix Isolation Infrared Spectroscopy. *Int. Rev. Phys. Chem.* **2008**, *27*, 1−25.
(49) Gong, Y.; Zhou, M. F.; Andrews, L. Spectroscopic and Theoretical Studies of Transition Metal Oxides and Dioxygen Complexes. *Chem. Rev.* **2009**, *109*, 6765−6808.
(50) Becke, A. D. Density-Functional Thermochemistry. III. The Role of Exact Exchange. *J. Chem. Phys.* **1993**, *98*, 5648−5652.
(51) Lee, C.; Yang, W.; Parr, R. G. Development of the Colle-Salvetti Correlation-Energy Formula into a Functional of the Electron-Density. *Phys. Rev. B: Condens. Matter Mater. Phys.* **1988**, *37*, 785−789.
(52) Frisch, M. J.; Trucks, G. W.; Schlegel, H. B.; Scuseria, G. E.; Robb, M. A.; Cheeseman, J. R.; Scalmani, G.; Barone, V.; Mennucci, B.; Petersson, G. A.; Nakatsuji, H.; Caricato, M.; Li, X.; Hratchian, H. P.; Izmaylov, A. F.; Bloino, J.; Zheng, G.; Sonnenberg, J. L.; Hada, M.; Ehara, M.; Toyota, K.; Fukuda, R.; Hasegawa, J.; Ishida, M.; Nakajima, T.; Honda, Y.; Kitao, O.; Nakai, H.; Vreven, T.; Montgomery, J. A.; Peralta, J. E.; Ogliaro, F.; Bearpark, M.; Heyd, J. J.; Brothers, E.; Kudin, K. N.; Staroverov, V. N.; Kobayashi, R.; Normand, J.; Raghavachari, K.; Rendell, A.; Burant, J. C.; Iyengar, S. S.; Tomasi, J.; Cossi, M.; Rega, N.; Millam, J. M.; Klene, M.; Knox, J. E.; Cross, J. B.; Bakken, V.; Adamo, C.; Jaramillo, J.; Gomperts, R.; Stratmann, R. E.; Yazyev, O.; Austin, A. J.; Cammi, R.; Pomelli, C.; W.Ochterski, J.; Martin, R. L.; Morokuma, K.; Zakrzewski, V. G.; Voth, G. A.; Salvador, P.; Dannenberg, J. J.; Dapprich, S.; Daniels, A. D.; Farkas, O.; Foresman, J. B.; Ortiz, J. V.; Cioslowski, J.; Fox, D. J. *Gaussian 09*, Revision A.1; Gaussian, Inc.: Wallingford, CT, 2009.
(53) Dunning, T. H. Gaussian basis sets for use in correlated molecular calculations. I. The atoms boron through neon and hydrogen. *J. Chem. Phys.* **1989**, *90*, 1007−1023.
(54) Peng, C.; Ayala, P. Y.; Schlegel, H. B.; Frisch, M. J. Using redundant internal coordinates to optimize equilibrium geometries and transition states. *J. Comput. Chem.* **1996**, *17*, 49−56.
(55) Raghavachari, K.; Trucks, G. W.; Pople, J. A.; Head-Gordon, M. A Fifth-Order Perturbation Comparison of Electron Correlation Theories. *Chem. Phys. Lett.* **1989**, *157*, 479−483.
(56) Zubarev, D. Y.; Boldyrev, A. I. Developing paradigms of chemical bonding: adaptive natural density partitioning. *Phys. Chem. Chem. Phys.* **2008**, *10*, 5207−5217.
(57) Lu, T.; Chen, F. W. Multiwfn: A multifunctional wavefunction analyzer. *J. Comput. Chem.* **2012**, *33*, 580−592.
(58) Fitzmaurice, D. J.; Frei, H. Photochemistry of Cycloalkene-NO_2 Collisional Pairs in a Cryogenic Matrix: Chemical Trapping of Cycloalkene Oxirane Biradical Conformers, and Comparison of Product Control for Excitation above and below the NO_2 Dissociation Threshold. *J. Phys. Chem.* **1991**, *95*, 2652−2661.
(59) Hannachi, Y.; Hassanzadeh, P.; Andrews, L. Ab Initio Study of the Insertion Product of the Boron-Methane Reaction: CH_3BH. *J. Phys. Chem.* **1994**, *98*, 6950−6954.
(60) Hoops, M. D.; Ault, B. S. Matrix isolation study of the photochemical reaction of cyclohexane, cyclohexene, and cyclopropane with ozone. *J. Mol. Struct.* **2009**, *929*, 22−31.
(61) Qin, C. Y.; Davis, S. R. Thermal Isomerization of Tricyclo[4.1.0.$0^{2,7}$]heptane and Bicyclo[3.2.0]hept-6-ene through the (E,Z)-1,3-Cycloheptadiene Intermediate. *J. Org. Chem.* **2003**, *68*, 9081−9087.
(62) Boldyrev, A. I.; Wang, L.-S. Beyond organic chemistry: aromaticity in atomic clusters. *Phys. Chem. Chem. Phys.* **2016**, *18*, 11589−11605.
(63) Sergeeva, A. P.; Popov, I. A.; Piazza, Z. A.; Li, W. L.; Romanescu, C.; Wang, L. S.; Boldyrev, A. I. Understanding boron through size-selected clusters: structure, chemical bonding, and fluxionality. *Acc. Chem. Res.* **2014**, *47*, 1349−1358.
(64) Feixas, F.; Matito, E.; Poater, J.; Sola, M. Quantifying aromaticity with electron delocalisation measures. *Chem. Soc. Rev.* **2015**, *44*, 6434−6451.
(65) Ocola, E. J.; Laane, J. Spectroscopic and theoretical study of the intramolecular π-type hydrogen bonding and conformations of 3-cyclohexen-1-ol. *J. Mol. Spectrosc.* **2022**, *387* (111663), 111663.
(66) Poland, K. N.; Yang, W. W.; Fortenberry, R. C.; Davis, S. R. The thermal isomerization of benzvalyne to benzyne. *Phys. Chem. Chem. Phys.* **2022**, *24*, 14573−14578.
(67) Veals, J. D.; Davis, S. R. Isomerization barriers for the disrotatory and conrotatory isomerizations of 3-aza-benzvalene and 3,4-diaza-benzvalene to pyridine and pyridazine. *Phys. Chem. Chem. Phys.* **2013**, *15*, 13593−13600.
(68) Christl, M.; Braun, M.; Deeg, O. Photochemical reactions of tetrachloro-1,4-benzoquinone (chloranil) with tricyclo[4.1.0.$0^{2,7}$]-heptane (Moore's hydrocarbon) and bicyclo[4.1.0]-hept-2-ene (2-norcarene). *Org. Biomol. Chem.* **2013**, *11*, 2811−2817.

https://doi.org/10.1021/jacsau.4c00492
JACS Au 2024, 4, 3183−3193